

Photoemission study of the formation of SrF₂/GaAs(100) and BaF₂/GaAs(100) interfaces

K. M. Colbow, Y. Gao, and T. Tiedje*

Physics Department, University of British Columbia, Vancouver, British Columbia, Canada V6T 1Z1

W. Eberhardt

Institut für Festkörperforschung, Forschungszentrum Jülich GmbH, Postfach 1913, D-52425 Jülich, Germany

(Received 30 November 1992)

Thin films of SrF₂ and BaF₂ grown on clean GaAs(100) surfaces have been studied by high-resolution photoemission spectroscopy. Similar to the previously studied CaF₂/GaAs(100) interface, there is evidence of cation-substrate bonding after annealing at temperatures near 600°C. For BaF₂, Ba was found to react with As at the interface with an associated loss of Ga and F. For SrF₂, the Sr 3*d* core-level shift also suggests cation-substrate bonding. The valence-band maxima for GaAs and the respective alkaline-earth fluorides (CaF₂, SrF₂, BaF₂) were measured directly by linear extrapolation of the high-kinetic-energy edge of the respective valence bands. The resulting valence-band offsets were found to follow the same trend for coverages up to 2–4 monolayers.

I. INTRODUCTION

Epitaxial growth of the alkaline-earth fluorides on elemental^{1–4} and compound semiconductors^{4–9} has attracted attention recently because of possible applications in some technologically important areas. Such insulator-on-semiconductor structures are potentially useful in multilevel-integrated-device structures and in optoelectronics. The three alkaline-earth fluorides CaF₂, SrF₂, BaF₂, and their alloys can be lattice matched to a broad range of III-V compounds including GaAs, InP, and InAs. The electronic and thermal stability of these interfaces are crucial in determining the suitability of these heterostructures for device applications. Together with CaF₂ on Si, CaF₂ on GaAs has been a useful model system for studying these ionic-covalent interfaces.

The interfaces of CaF₂ and SrF₂ with Si have been studied with a variety of techniques including ultraviolet photoemission spectroscopy,^{2,3} medium-energy ion scattering,¹⁰ and transmission electron microscopy.¹¹ Film morphology and crystallinity, interface bonding, and electronic properties such as the Fermi-level pinning and valence-band offset have been determined for these interfaces. Several discussions of the CaF₂/Si(111) structure assumed that the CaF₂ molecule remained intact at the interface with a Si-(F-Ca-F)_n layer sequence. However, there is now general agreement that the high-temperature-growth interface is not stoichiometric, but rather consists of direct Si-Ca bonds.¹² The valence-band offsets for these interfaces ranged between 7.3 and 8.3 eV as determined from valence-band photoemission spectra.²

Epitaxial growth of CaF₂ has been achieved on GaAs.^{4–9} Recently, the CaF₂/GaAs(110) and SrF₂/GaAs(110) interfaces, formed by deposition of amorphous films at room temperature on cleaved GaAs(110) surfaces, have been studied by photoemission spectroscopy.⁷ Core-level measurements indicated that no

reaction or decomposition of the MF₂ molecule takes place at the interface. Contrary to the CaF₂/Si case, no measurable Ca-substrate bonding is observed, but the data suggest the presence of an interface F component. The band offsets were found to be in qualitative agreement with those expected from the fluoride-Si data.

A systematic photoemission study of the effects of thermal annealing on the interfacial composition and bonding for CaF₂ deposited on GaAs(100) at room temperature has also been reported.⁹ The CaF₂ thin films were deposited in ultrahigh vacuum by evaporation on clean GaAs(100), and subsequently annealed in steps up to 590°C. By 550°C, a monolayer of Ca was found to react with As at the interface with an associated loss of approximately one Ga and one F by evaporation per formula unit of CaF₂. The thickness of the interfacial layer was found to terminate at one monolayer for the given range of annealing conditions. Contrary to the CaF₂/GaAs(110) interfaces formed at room temperature,⁷ in our studies of the CaF₂/GaAs(100) interface no evidence for F-substrate bonding was observed. The interfacial valence-band offset was found to be 8.5 eV and the Fermi level approached the GaAs valence-band edge with increasing CaF₂ overlayer thickness.

In this paper we report results of a similar systematic high-resolution photoemission study of the effects of thermal annealing on the interfacial composition and bonding, and the valence-band offset, for SrF₂ and BaF₂ deposited on GaAs(100) at room temperature and subsequently annealed. The data for the SrF₂/GaAs and BaF₂/GaAs systems are more difficult to interpret because of the relatively small cross sections of the Sr- and Ba-related spectral features as compared to Ca, and because of their overlap with the spectral features of the GaAs substrate. However, from our understanding of the CaF₂/GaAs interface, certain similarities in these systems can be identified, and thus, conclusions can be drawn concerning the interface formation.

II. EXPERIMENT

The experiments were carried out at the U1 beamline¹³ at the National Synchrotron Light Source, Brookhaven National Laboratory. Samples of semi-insulating liquid-encapsulated-Czochralski-type GaAs(100) wafers were mounted in Ta-foil baskets spot welded to Ta wires, which could be heated resistively. The sample and/or basket temperature was measured with an infrared pyrometer that had been previously calibrated.⁹ Prior to fluoride deposition, the GaAs surfaces were cleaned by heating to desorb the surface oxides followed by soft Ar⁺ sputtering (500 eV) and annealing (550°C) cycles until no residual carbon was detectable in photoemission. Preparation of GaAs(100) surfaces in this fashion are known¹⁴ to give low-energy electron diffraction patterns showing a sharp, low-background 4×2 reconstruction and corresponds to that of a well-ordered Ga-terminated surface. We also found no changes in the Ga 3*d*-to-As 3*d* photoemission intensity ratio or in the Ga 3*d* and As 3*d* chemical shifts during the sputter and/or anneal process, confirming that the surfaces are stoichiometric. A small amount of excess Ga is easily detected in photoemission by the characteristic chemical shift in the Ga 3*d* core level corresponding to Ga-Ga bonding.

The clean substrates were transferred under ultrahigh vacuum to a separate chamber, where powders of the alkaline-earth fluorides were evaporated at rates of 0.2–0.6 Å/s from Ta boats in a background pressure of $\leq 6 \times 10^{-9}$ mbar. These group-II fluorides sublime without dissociation of the MF₂ molecule leading to deposited films that are stoichiometric. A quartz-crystal thickness monitor was used for relative thickness measurements during deposition. After deposition, the fluoride films were annealed at progressively higher tem-

peratures for 1 min intervals in a range from 370°C to 630°C.

The thickness of the deposited films was estimated from the ratio of the integrated intensity of the respective cation (Sr 4*p* and Ba 5*p*) and F 2*p* photoemission peaks to the intensity of the Ga 3*d* peak from the underlying substrate, as described previously.⁹ Assuming that the fluoride overlayer has thickness *d* and is laterally homogeneous, the ratio of the intensity of an overlayer core level to the Ga 3*d* substrate core level is

$$R = K \left\{ \frac{1 - e^{-d/\lambda}}{e^{-d/\lambda}} \right\}, \quad (1)$$

where *K* is a constant expressing the relative cross sections of the overlayer and substrate photoemission peaks and λ is the escape depth of the photoelectrons in the alkaline-earth fluorides. In this analysis we assume the escape depth for 50–100 eV photoelectrons in the fluorides to be 6 Å.⁹ For CaF₂, the constant *K* in Eq. (1) was determined from the absolute-peak intensities for clean GaAs substrates and thick CaF₂ overlayers. For SrF₂ and BaF₂, the constants *K* were scaled in accordance with the photoionization cross sections as determined by Yeh and Lindau¹⁵ for photon energies in the 80–90 eV range. The resulting values of *K* for the three alkaline-earth fluorides and the photoionization cross sections are summarized in Table I. These values of *K*, together with the measured peak intensity ratio *R* and the assumed value of λ , were then used to determine the fluoride-film thickness *d* from Eq. (1). The experimental uncertainty in the determination of *K* contributes a 20% uncertainty to the film thickness. One monolayer (ML) of MF₂ on GaAs(100) is defined as one MF₂ molecule per surface atom and these values are also shown in Table I.

TABLE I. Lattice constants, lattice mismatch, energy gap, photoionization cross sections, and *K* values for the alkaline-earth fluorides and GaAs.

	CaF ₂		SrF ₂		BaF ₂		GaAs	
Lattice constant <i>a</i> (Å) ^a	5.451		5.784		6.187		5.6537	
Lattice mismatch (%)	−3.6		2.3		9.4			
1 ML (Å)	3.15 ^b		3.34 ^c		3.58 ^c			
	Ca 3 <i>p</i>	F 2 <i>p</i>	Sr 4 <i>p</i>	F 2 <i>p</i>	Ba 5 <i>p</i>	F 2 <i>p</i>	Ga 3 <i>d</i>	As 3 <i>d</i>
Photoionization cross sections (Mb) ^d (<i>hν</i> = 83.6 eV)	1.5	3.4	0.4	3.4	0.37	3.4	8.5	5.5
	Ca/Ga	F/Ga	Sr/Ga	F/Ga	Ba/Ga	F/Ga		
K values	1.17	4.66	0.31	4.66	0.29	4.66		
Energy gap <i>E_g</i> (eV) ^e	12.1		11.25		11.0		1.42	

^aReference 20.

^bValue from Ref. 3.

^cValue scaled with lattice constant from Ref. 3.

^dReference 15.

^eReference 21.

III. RESULTS AND DISCUSSION

A. BaF₂

Figure 1 shows photoelectron spectra measured with a photon energy of 83.6 eV for a series of anneals of 3.8 ML of BaF₂ deposited at room temperature on GaAs(100) showing the As 3*d*, Ba 5*s*, F 2*s*, Ga 3*d*, Ba 5*p*, and F 2*p* photoemission features. The Ba *NVV* Auger peak also contributes to the broad spectral feature in the 45–50 eV kinetic-energy range of these spectra. It is apparent that the photoemission features of the substrate are clearly enhanced relative to those of the BaF₂ overlayer at higher annealing temperatures. This indicates a decrease in the overlayer thickness with increasing annealing temperature, possibly due to the decomposition of BaF₂ at the interface. Alternatively, high-temperature annealing may cause the BaF₂ film to nucleate and form three-dimensional islands on the semiconductor surface. For CaF₂, this latter explanation was shown not to be the case, as an exponential decrease in the ratio of the Ga 3*d*–to–F 2*p* photoemission peak area was observed, consistent with the formation of uniform CaF₂ films. Because of the larger lattice mismatch between GaAs and BaF₂, compared to CaF₂, it is possible that the BaF₂ films form islands on the substrate surface.

The Ga 3*d* and Ba 5*p* core levels from the spectra in Fig. 1 were fitted in order to determine the nature of the chemical bonding at the interface, and the results of these fits are shown in Fig. 2. The Ga 3*d* core level was fit with a 0.45-eV spin-orbit split doublet and a branching ratio of 1.6 as determined previously by Ludeke, Chiang, and Eastman.¹⁶ The Ba 5*p* core level was similarly fit with doublets spin-orbit split by 2.06 eV and a branching ratio of 2.5. These values were experimentally determined by

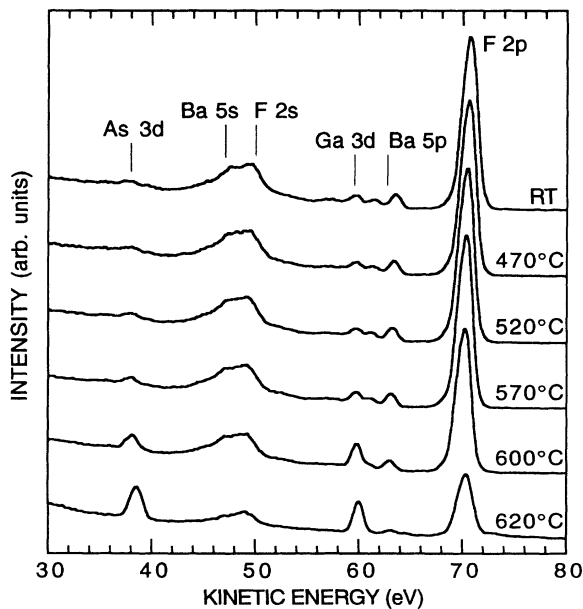


FIG. 1. Photoemission spectra for 3.8 ML of BaF₂ on GaAs for a series of annealing temperatures from 470°C to 620°C measured with a photon energy of 83.6 eV.

fitting the Ba 5*p* core level for a thick BaF₂ film. The value for the spin-orbit splitting agrees well with previous values for elemental Ba.¹⁷ The variation of the branching ratio for the Ba 5*p* and La 5*p* core levels has been previously studied by Ichikawa *et al.*,¹⁸ and our value of 2.5 at a photon energy of 83.6 eV is in agreement with their results. The deviation of the branching ratio from the statistical value of 2 has been attributed to a difference in the relative strength of the coupling between the 5*p*_{1/2} and 5*p*_{3/2} hole states with the *d*-like electron wave of the photoemission final state. This *p*-*d* coupling results from the nonradiative (participator¹⁹) decay of 4*d*⁹4*f*¹ excited states of the cations which are excited in the 80–100-eV photon-energy range, where a 4*d* hole and excited electron recombine directly, whereby the energy is transferred to a 5*s* or 5*p* electron of the cation.¹⁸

The peaks were fitted using Lorentzian line shapes convoluted with Gaussians of 0.3 eV width modeling the experimental resolution. The fitting parameters were the Lorentzian peak widths, positions, and intensities. From Fig. 2, we see that the Ba 5*p*/Ga 3*d* photoemission inten-

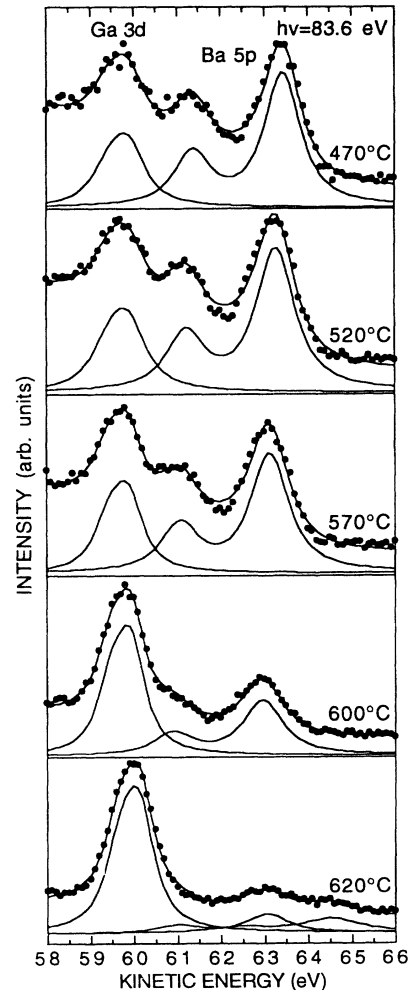


FIG. 2. Fitted photoemission spectra of the Ga 3*d* and Ba 5*p* region of the core level for the series of annealing temperatures for the sample of Fig. 1.

sity ratio decreases by almost a factor of 5. This is thought to be partially due to the formation of islands on the substrate surface, but at the higher annealing temperatures is attributed to BaF_2 decomposition. Also, at the highest annealing temperature, a chemically shifted component of the Ba $5p$ core level is observed. This shift is 1.5 eV towards lower binding energy. We interpret the major Ba $5p$ component to be the ionic Ba^{2+} species in bulk BaF_2 . This means the chemically shifted component of the Ba $5p$ core level in the bottommost spectrum is due to Ba ions that are in a lower-nominal-oxidation state than the Ba^{2+} ions in BaF_2 . In analogy with the CaF_2/GaAs system,⁹ where a comparable 1.8-eV chemically shifted component was observed at higher annealing temperatures, we attribute this relatively large chemically shifted component to Ba at the interface. In contrast, the Ga $3d$ core level exhibits no visible chemical shift, in fact the peak width remains constant within the uncertainty of the fitting procedure.

The relatively strong Ba $4d$ core level was also measured for this sample at a photon energy of 160.9 eV. This choice in photon energy resulted in kinetic energies for the emitted electrons of approximately 60 eV, similar to those found for the Ba $5p$ core levels in the 83.6-eV photon-energy spectra. This ensured a similar degree of surface sensitivity for the Ba $5p$ and Ba $4d$ core-level spectra. The fitted Ba $4d$ core level as well as the As $3d$ core level are shown in Fig. 3. From a thick BaF_2 sample, the spin-orbit splitting of the Ba $4d$ core level was determined to be 2.68 eV with a branching ratio of 1.2. The value for the spin-orbit splitting compares well with previous values,¹⁷ and the deviation of the branching ra-

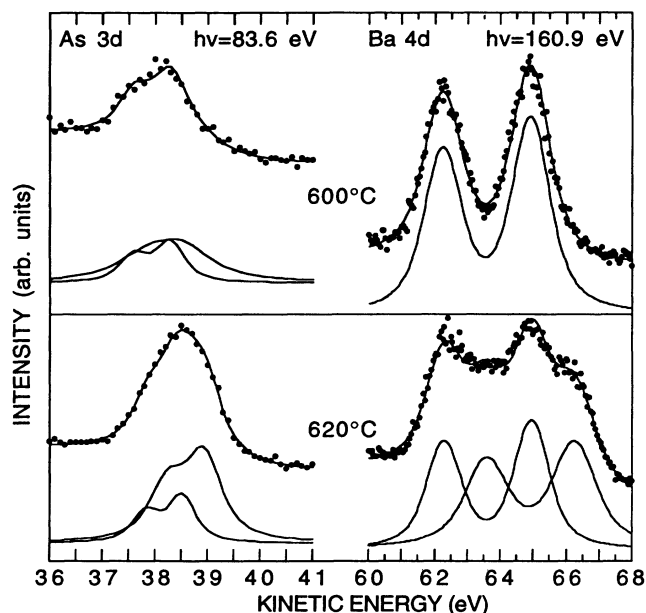


FIG. 3. Fitted photoemission spectra of the Ba $4d$ and As $3d$ core level for a series of annealing temperatures for the sample of Fig. 1. The Ba $4d$ core level was measured with a photon energy of 160.9 eV.

tio from the statistical value of 1.5 is partially attributed to the steep decrease in the photoionization cross section of the $4d$ core level in the 100–170-eV photon-energy range.¹⁵ Two spin-orbit doublets with these experimentally determined parameters were then used to fit the Ba $4d$ core levels. At 620°C, a chemical shift of approximately 1.3 eV toward lower binding energy is observed, similar to the one observed for the Ba $5p$ core level and thus we interpret it as the Ba species at the interface. Furthermore, the photoemission intensity ratios for the Ba interface peak to the bulk peak are equal in both cases to within experimental uncertainty, namely, 1.2 ± 0.2 .

The thickness of the BaF_2 film at the highest annealing temperature was determined from the Ba $5p/\text{Ga } 3d$ and F $2p/\text{Ga } 3d$ photoemission intensity ratios to be 1.8 and 1.1 ML, respectively. This discrepancy is attributed to the loss of F relative to Ba resulting from BaF_2 decomposition. Based on the relative photoemission intensity ratio of the Ba $4d$ interface component to the bulk component, it is evident that even at the highest annealing temperature, the interface does not uniformly consist of the Ba interface component. It is possible that 620°C is not hot enough to allow complete formation of the Ba interface component; however, it is also possible that the BaF_2 film has formed islands on the semiconductor surface. Furthermore, and in analogy to the CaF_2/GaAs system, we observe a decrease in both the F $2p/\text{Ba } 5p$ and the Ga $3d/\text{As } 3d$ intensity ratios and attribute these relative losses of Ga and F to the decomposition of BaF_2 at the interface, followed by the possible formation of a volatile GaF_x compound, which is lost by evaporation.

To further investigate the chemical bonding at the interface and to better understand the observed chemical shifts in the Ba core levels, the As $3d$ core levels from the spectra in Fig. 1 were also fitted and are shown in Fig. 3. The values of Ludeke, Chiang, and Eastman,¹⁶ namely, a spin-orbit splitting of 0.69 eV and a branching ratio of 1.53, were used for the As $3d$ core level. In both spectra in Fig. 3, the fitted component of the As $3d$ core level at higher binding energy corresponds to As in bulk GaAs. The component at lower binding energy corresponds to As at the interface. After annealing at 600°C, the interface As peak is broad and shifted by only 0.2 eV, similar to the surface core-level shift observed for clean GaAs(100),¹⁶ which is also slightly shifted to lower binding energy relative to the bulk peak. At 620°C, this component becomes much stronger and shifts to 0.4 eV lower binding energy relative to the bulk peak. We attribute this chemical shift to As chemically bonded to Ba at the interface.

Similar to the CaF_2/GaAs system,⁹ the cation (Ba) causes a shift to lower binding energy because it donates more charge to the adjacent As atoms than the Ga does, due to the lower electronegativity of Ba relative to Ga. A related chemical shift would be expected for the Ba $4d$ and $5p$ core levels due to the lower electronegativity of As relative to F. As shown in Figs. 2 and 3, these chemical shifts are observed and, together with the apparent loss of Ga and F at higher annealing temperatures, naturally lead to an interpretation of Ba-As bonding at the interface.

B. SrF₂

Figure 4 shows photoelectron spectra measured at a photon energy of 83.6 eV for a series of anneals for 2.5 ML of SrF₂ deposited at room temperature on GaAs(100) showing the As 3*d*, Sr 4*s*, F 2*s*, Sr 4*p*, Ga 3*d*, and F 2*p* photoemission features. Unlike the CaF₂/GaAs system⁹ and the BaF₂/GaAs system discussed above, the cation core levels from SrF₂, namely, the Sr 4*p* and Sr 4*s* levels, partially overlap with the strong photoemission features from the Ga 3*d* and As 3*d* core levels. From the results of the other two alkaline-earth fluorides studied, we expect chemically shifted components of the As 3*d* core level and the Sr core levels towards lower binding energy. Such results are difficult to interpret because of the overlap with the Sr 4*s* and Ga 3*d* core levels, respectively. Furthermore, as shown in Table I, the photoionization cross sections for the Sr 4*p* and Sr 4*s* core levels are weak compared to those of the Ca 3*p*, Ga 3*d*, or As 3*d* core levels. From Fig. 4, however, it is evident that at the higher annealing temperatures the spectral features associated with the GaAs substrate are clearly enhanced relative to those of the SrF₂ overlayer. Similar to the BaF₂/GaAs system, this indicates a decrease in the overlayer thickness with annealing temperature, possibly due to SrF₂ decomposition at the interface. One would expect that because of the smaller lattice mismatch with GaAs of SrF₂ compared to either CaF₂ or BaF₂, that the formation of three-dimensional islands at higher annealing temperatures would be unlikely, however this possibility cannot be ruled out.

As mentioned, the Sr 4*s* and 4*p* core levels contain little information concerning possible chemical shifts. Therefore, the relatively strong Sr 3*d* core level was also measured. Figure 5 shows the Sr 3*d* core level measured for

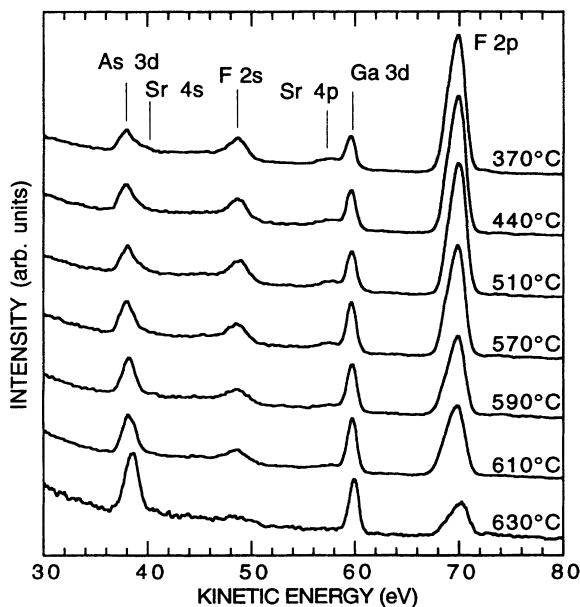


FIG. 4. Photoemission spectra for 2.5 ML of SrF₂ on GaAs(100) for a series of annealing temperatures from 370°C to 610°C measured with a photon energy of 83.6 eV.

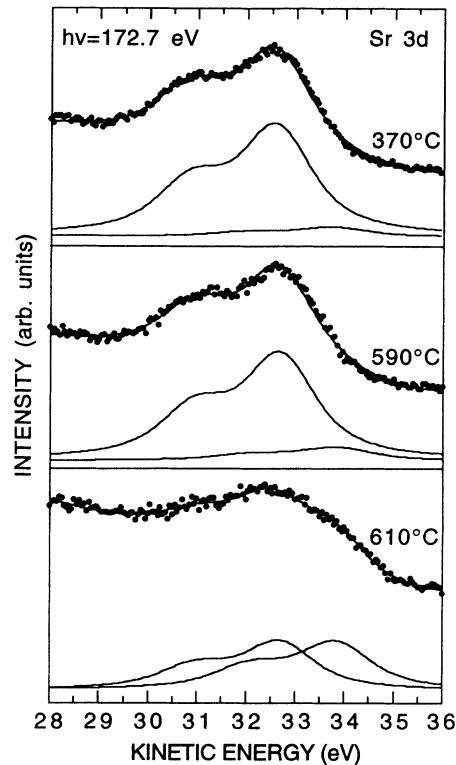


FIG. 5. Fitted photoemission spectra of the Sr 3*d* core level for a series of annealing temperatures for the sample of Fig. 4 measured with a photon energy of 172.7 eV.

several annealing steps of the sample of Fig. 4 at 172.7-eV photon energy. This choice of photon energy gives electron kinetic energies for the Sr 3*d* core level in the 30–40 eV range, thus ensuring similar surface sensitivities for both the Sr 3*d* and As 3*d* core levels. The Sr 3*d* core-level spectra were fitted with a 1.72 eV spin-orbit split doublet with a branching ratio of 2.1, as determined from a thick, bulklike SrF₂ film. The value for the spin-orbit splitting compares well with previous values.¹⁷ The deviation of the branching ratio from the statistical value of 1.5 is partially attributed to the steep increase in photoionization cross section of the 3*d* core level in the 140–180 eV photon-energy range.¹⁵ The Lorentzian peaks with the above parameters were convoluted with a Gaussian 0.8-eV wide, which took into account the overall experimental resolution of the monochromator and energy analyzer in this photon-energy range. We interpret the larger component at higher binding energy in these fits as Sr²⁺ cations from bulk SrF₂. At the higher annealing temperatures, the Sr 3*d* core level exhibits a second component, shifted by approximately 1.1 eV towards lower binding energy. After annealing at 610°C, this shifted component becomes approximately equal in intensity with the bulk component. In analogy with the CaF₂ and BaF₂ systems, we interpret this as Sr at the interface, which is in a different chemical environment than in bulk SrF₂.

Again no chemical shift was observed in the Ga 3*d* photoemission peak. For the As 3*d* core level, however, a

chemical shift appears to be present at approximately 590°C, although this shift would be in exactly the position of the Sr 4s core level making a conclusive interpretation difficult. The trend in the ratios of the area of the F 2p/Sr 4p and Ga 3d/As 3d photoemission peaks is also difficult to determine because of the overlapping core levels, however qualitatively, the Ga/As ratio decreases in a similar way as previously observed for the CaF₂ and BaF₂ systems. As a result, the data presented in Figs. 4 and 5 are consistent with the bonding model for the CaF₂/GaAs system⁹ and the BaF₂/GaAs system discussed above.

C. Valence-band offsets

Figure 6 shows the valence-band offset as a function of overlayer thickness for SrF₂ and BaF₂ together with earlier results⁹ for CaF₂. The valence-band maxima for GaAs and the respective alkaline-earth fluoride overlayers are measured directly by linear extrapolation of the sharp edges on the high-kinetic-energy side of the respective valence bands. This procedure is straightforward due to the large energy separation of the two valence-band edges. All the data points in Fig. 6 are from interfaces that had been annealed to at least 400°C and some as high as 600°C. For CaF₂ overlayers, the valence-band offset ΔE_v decreases by more than 1.5 eV as the thickness of the CaF₂ is reduced. For SrF₂ and BaF₂ overlayers, the thickness dependence of ΔE_v is consistent with the CaF₂ results over the thickness range where the data overlap. However, the data on SrF₂ and BaF₂ in Fig. 6 are less extensive than for CaF₂ and we are unable to show that the thickness dependence is the same over the entire, larger thickness range, explored for CaF₂.

As shown in Table I, the band gaps of SrF₂ and BaF₂ are slightly smaller than the CaF₂ band gap. Similarly, for a given film thickness, the band offsets for SrF₂ and

BaF₂ also appear to be smaller by approximately the same amount. This result holds true for coverages up to 2–4 monolayers. Although, due to quantum size effects, it is not correct to equate band gaps of the bulk material to the band gaps of monolayer thicknesses, these measured valence-band offsets lead to conduction-band offsets which, to within the uncertainty of these measurements, are equal for the three alkaline-earth fluorides.

The scatter in the band offsets in Fig. 6 is not associated with the annealing temperature. For example, if the band offsets for the nine SrF₂ samples near two monolayers in thickness in Fig. 6 are plotted as a function of the annealing temperature, there is no correlation with the annealing temperature, as shown in Fig. 7. The scatter is consistent with the measurement uncertainty. The lack of dependence on annealing temperature is not an obvious result in view of the interfacial compound formation, which takes place with annealing as discussed above. Two physical mechanisms could contribute to the observed change in the band offset with thickness for CaF₂. The first is a strain-induced change in the band offset resulting from a possible structural evolution as the overlayer thickness increases through the first few monolayers due to the 3.6% lattice mismatch between GaAs and CaF₂. Although difficult to quantify without more detailed structural information of the overlayer as a function of thickness, a similar mechanism could apply for SrF₂ (2.3% mismatch) and BaF₂ (9.4% mismatch).

The second effect that would cause the measured apparent band offset to change with thickness is changes in the energy band structure of the alkaline-earth fluorides as the layer thickness approaches a single monolayer. Interactions with the semiconductor could also modify the energy-level structure of a monolayer thick film. In any case, these results are consistent with the valence-band offsets of 7.7 ± 0.3 and 7.6 ± 0.3 eV reported earlier for 1–2 ML of CaF₂ and SrF₂ deposited at room temperature on GaAs(110), respectively.⁷

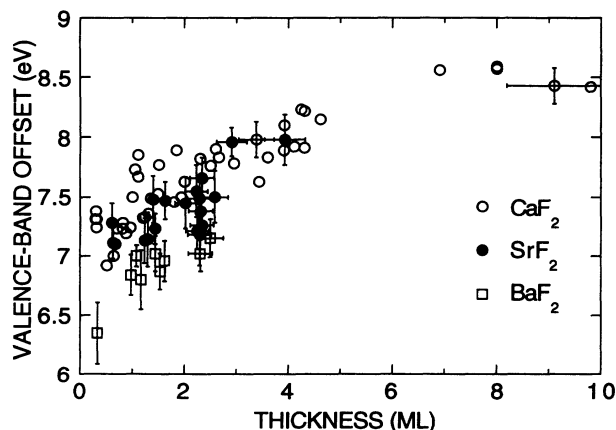


FIG. 6. Compilation of the valence-band offsets as a function of overlayer thickness for the alkaline-earth fluoride/GaAs(100) interfaces. For clarity, error bars are displayed for all the SrF₂ and BaF₂ data points. The experimental uncertainty in the data points for CaF₂ are similar.

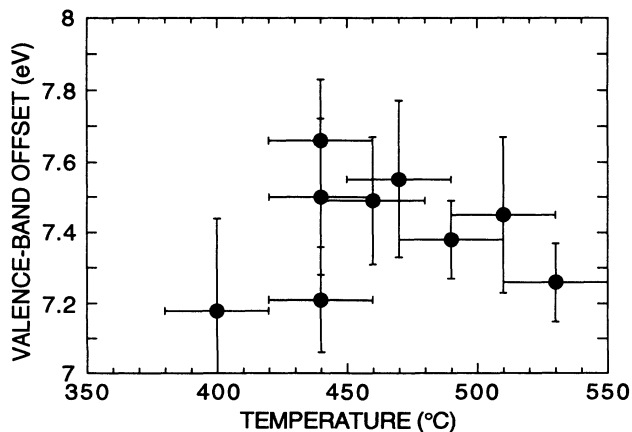


FIG. 7. Valence-band offsets for the nine SrF₂ samples near two monolayers in thickness in Fig. 6 as a function of the annealing temperature.

IV. SUMMARY AND CONCLUSIONS

The interfacial bonding and energy-band alignments have been measured for the SrF₂ and BaF₂ interface with GaAs(100) as a function of annealing temperature by high-resolution photoemission spectroscopy. Similar to the previously studied CaF₂/GaAs(100) interface, there is evidence of cation-substrate bonding at temperatures near 600°C. For the BaF₂/GaAs(100) interface, Ba was found to react with As at the interface with an associated loss of Ga and F. For SrF₂, the Sr 3*d* core-level shift also suggested cation-substrate bonding; however, due to the overlap in energy position of substrate and overlayer core levels a more conclusive interpretation for this system is difficult. In any case, given that the three alkaline-earth fluorides have very similar chemical and electronic prop-

erties, it is not surprising that their interfaces with GaAs(100) display similar interfacial bonding properties. The valence-band maxima for GaAs(100) and the respective alkaline-earth fluorides (CaF₂, SrF₂, BaF₂) were measured directly by linear extrapolation of the high-kinetic-energy edge of the respective valence bands. The resulting valence-band offsets were found to follow the same trend for coverages up to 2–4 monolayers.

ACKNOWLEDGMENTS

We thank the Natural Sciences and Engineering Research Council of Canada for financial support. This research was carried out at the National Synchrotron Light Source, Brookhaven National Laboratory, a U. S. Department of Energy facility.

*Also at Electrical Engineering Department, University of British Columbia, Vancouver, British Columbia, Canada V6T 1Z1.

- ¹J. M. Phillips, L. C. Feldman, J. M. Gibson, and M. L. McDonald, *Thin Solid Films* **107**, 217 (1983).
- ²M. A. Olmstead, R. I. G. Uhrberg, R. D. Bringans, and R. Z. Bachrach, *Phys. Rev. B* **35**, 7526 (1987).
- ³D. Rieger, F. J. Himpsel, U. O. Karlsson, F. R. McFeely, J. F. Morar, and J. A. Yarmoff, *Phys. Rev. B* **34**, 7295 (1986).
- ⁴S. Sinharoy, *Thin Solid Films* **187**, 231 (1990).
- ⁵S. Siskos, C. Fontaine, and A. Munoz-Yague, *J. Appl. Phys.* **56**, 1642 (1984).
- ⁶S. Sinharoy, F. A. Hoffman, J. H. Rieger, R. F. C. Farrow, and A. J. Noreika, *J. Vac. Sci. Technol. A* **3**, 842 (1985).
- ⁷D. Mao, K. Young, A. Kahn, R. Zanoni, J. McKinley, and G. Margaritondo, *Phys. Rev. B* **39**, 12 735 (1986).
- ⁸Y. Yamada, M. Oshima, T. Waho, T. Kawamura, S. Maeyama, and T. Miyahara, *Appl. Surf. Sci.* **41/42**, 647 (1989); T. Waho, F. Yanagawa, and Y. Yamada, *J. Cryst. Growth* **95**, 415 (1989).
- ⁹K. M. Colbow, T. Tiedje, D. Rogers, and W. Eberhardt, *Phys. Rev. B* **43**, 9672 (1991).
- ¹⁰R. M. Tromp and M. C. Reuter, *Phys. Rev. Lett.* **61**, 1756 (1988).
- ¹¹J. L. Batstone, J. M. Phillips, and E. C. Hunke, *Phys. Rev. Lett.* **60**, 1394 (1988).
- ¹²M. A. Olmstead and R. D. Bringans, *Phys. Rev. B* **41**, 8420 (1990).
- ¹³M. Sansone, R. Hewitt, W. Eberhardt, and D. Sondericker, *Nucl. Instrum. Methods A* **266**, 422 (1988).
- ¹⁴See, for example, J. E. Ortega and F. J. Himpsel, *Phys. Rev. B* **47**, 2130 (1993); M. D. Pashley, K. W. Habernern, W. Friday, J. W. Woodall, and P. D. Kirchner, *Phys. Rev. Lett.* **60**, 2176 (1988); P. Drathen, W. Ranke, and K. Jacobi, *Surf. Sci.* **77**, L162 (1978); A. J. van Bommel, J. E. Crombeen, and T. G. J. van Oirschot, *ibid.* **72**, 95 (1978).
- ¹⁵J. J. Yeh and I. Lindau, *At. Data Nucl. Data Tables* **32**, 1 (1985).
- ¹⁶R. Ludeke, T. C. Chiang, and D. E. Eastman, *Physica* **117B-118B**, 819 (1983).
- ¹⁷*Photoemission in Solids I; General Principles*, edited by M. Cardona and L. Ley (Springer-Verlag, Berlin, 1978); J. C. Fuggle and N. Mårtensson, *J. Electron Spectrosc. Relat. Phenom.* **21**, 275 (1980).
- ¹⁸K. Ichikawa, O. Aita, K. Aoki, M. Kamada, and K. Tsutsumi, *Phys. Rev. B* **45**, 3221 (1992).
- ¹⁹T. Tiedje, K. M. Colbow, D. Rogers, and W. Eberhardt, *Phys. Rev. Lett.* **65**, 1243 (1990).
- ²⁰R. W. G. Wyckoff, *Crystal Structures*, 2nd ed. (Wiley, New York, 1963 and 1964), Vols. 1 and 2.
- ²¹G. W. Rubloff, *Phys. Rev. B* **5**, 662 (1972).